Analysis of JT-60U Divertor Plasma Using "B2-Eirene" Code

A.Hatayama[*1], R.Schneider[*2], D.P.Coster[*2],
N.Hayashi[*1,*4], M.Sugihara[*3], M.Ogasawara[*1],
K.Shimizu[*4], N.Asakura[*4] and T.Hirayama[*4]
*1: Faculty of Science and Technology, Keio University Yokohama 223, Japan
*2: Max-Planck-Institut fur Plasmaphysik, Garching, FRG.
*3: ITER JCT, IPP Garching,
*4: Japan Atomic Energy Research Institute, Naka, Ibaraki, Japan

1. Introduction "B2-Eirene" code [1-4] has been successfully applied to the analyses for the present divertor experiments and the predictive study for the future reactors. The present study is the first attempt to apply the "B2-Eirene" code to the analysis of JT-60U divertor plasma. In Ref.[5], extensive studies of recycling, particle flux and divertor plasma parameters have been made for JT-60U L-mode discharges. The relation between total recycling particle flux and the main plasma parameters, such as NBI heating power P_{NBI}, effective safety factor q_{eff}, line averaged electron density $\bar{n}_e$, has been investigated for the wide range of experimental condition. Comparison of "B2-Eirene" results with the above global feature of particle flux in JT-60U has been done in this study. In addition, we compare numerical results for n_e, T_e and CII-line radiation profiles in the SOL/divertor region with the experimental results, taking a JT-60U shot (shot#E19059) [6] as an example.

2. Numerical Model The main aspects of "B2-Eirene" code package have been described in detail in Refs.[1-4]. Here, we briefly summarize numerical model used in the present study. Bulk ion species D^+ and all carbon impurity ion species (C^+-C^{6+}) are described by the "B2" multi-fluids code[2]. This plasma description is self-consistently coupled[1] to the "Eirene" Monte-Carlo-code[3],[4] for the neutrals. Essential features of neutral kinetics for D, D_2 and C are taken into account. Figure 1 shows JT-60U configuration and numerical grid. Sight lines of optical fiber array (38 ch.) are also shown in Fig.1. MHD equilibrium data for the grid generation is taken from the shot#E19059 (I_p=2MA, B_t=4T, and q_{eff}=5.05). Time evolution of this example shot (#E19059) is shown in Fig.2 from Ref.[6]. We use

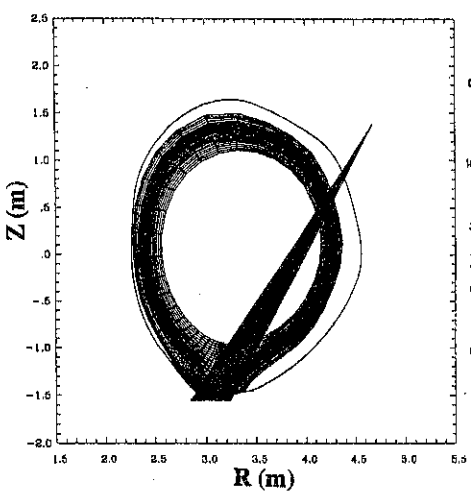

Fig.1 JT-60U configration and numerical grid

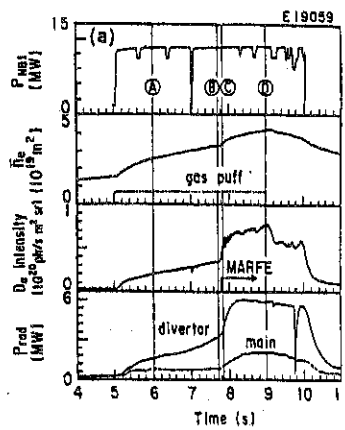

Fig.2 Time history of shot #E19059 (from Ref.[6])

constant transport coefficient model for anomalous radial transport. Three different cases [(a):D=1.0m^2/s, χ_e=χ_i=0.3m^2/s, (b):D=1.0m^2/s, χ_e=χ_i=2.0m^2/s, (c): D=0.5m^2/s, χ_e=χ_i=2.0m^2/s] have been considered. Taking into account loss mechanisms in the main plasma, we set total input power as P_{in}=9MW throughout this study and equally distributed in the cells at inner most flux surface in Fig.1. The remaining set of boundary conditions is the almost same as those in Ref.[1].

3. Global feature of particle flux In Ref.[5], the relation between total particle flux Φ^D and the main plasma parameters has been investigated for wide range of experimental conditions. As shown in Fig.3[5], Φ^D has been scaled as $\Phi^D = C_1 exp(\bar{n}_e q_{eff}/C_2)$, where C_1 and C_2 are the fitting parameters and depend mainly on geometrical factor, e.g., plasma volume, X-point height. Before proceeding to the detailed comparison with the shot #E19059, we have done the preliminary density scan in order to compare with the above global feature. In this series of run, deuterium density at bulk plasma side has been changed as n_D=0.5, 1.0, 2.0, 3.0 and 3.5 x10^{19}m^{-3}, respectively. For the radial transport coefficients, the case(a) above has been used. Since the numerical grid shown in Fig.1 is produced from the MHD equilibrium for shot#E19059, magnetic configuration is not exactly the same as those in Fig.3. However, plasma parameters of $I_p = 2MA$, $B_t = 4T$ and $q_{eff} = 5.05$ are very similar and also P_{in} (=9MW) is within the range of experimental parameter scan in Fig.3. Figure 4 shows the "B2-Eirene" results. In Fig.4, Φ^D at the divertor plate is plotted as a function of $n_e^{sep} q_{eff}$ instead of $\bar{n}_e q_{eff}$, where n_e^{sep} is calculated separatrix electron density at the outer mid-plane. Basically the same tendency as in Fig.3 can be seen. The total particle flux Φ^D increases almost linearly with $n_e^{sep} q_{eff}$ in logarithmic scale, expect for the highest density case. In the highest density case, main radiated region by the carbon was not localized in the divertor region, but near X-point inside the separatrix. Therefore, this highest density case is close to Marfe onset(or in the Marfe state, depending on the definition of Marfe). In order to make more exact comparison with Fig.3, the relation between n_e^{sep} and $\bar{n}_e$ is needed. If we roughly assume $\alpha = \bar{n}_e / n_e^{sep} = 2.5$ from Thomson scattering data at r/a =0.97, the "B2-Eirene" results in Fig.4 can be re-plotted as a function of $\bar{n}_e q_{eff}$ and well fitted by $\Phi^D = C_1 exp(\bar{n}_e q_{eff}/C_2)$ with

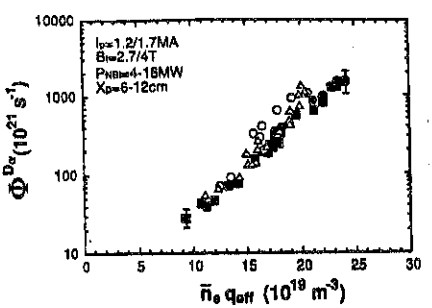

Fig.3 Φ^Das a function of $\bar{n}_e q_{eff}$

(from Ref.[5])

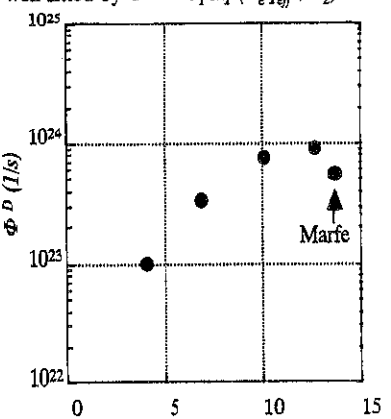

Fig.4 Depenedence of Φ^D on $n_e^{sep} q_{eff}$

C_1 = 30.0 and C_2 = 8.7. Compared with the experimental fit, C_2 is quite close, while C_1 is about 2.5 times larger. However, above fitting is based on the crude estimate for α and α is fixed constant for all n_D. Generally, α becomes smaller as density increases. If we take account of this feature, more close agreement can be obtained.

4. Analysis of shot#E19059 In the present study, we concentrate on the low density phase "A" in Fig.2. For this low density phase, we set as n_D=0.5x10^{19}m^{-3}. Figure 5 shows T_e profile at the outer mid-plane as a function of the distance d from the separatrix. Curve (a) and (b) correspond to the result for the different transport, the case (a) and the case (b) in Sec.2, respectively. In both cases, T_e drops quickly from the separatrix but then decreases more gradually. A long tail, i.e., a "second SOL" is formed. This behavior can be explained by the strong dependence of parallel classical heat diffusivity $\chi_{//}$ on T_e and consistent with theoretical prediction[7]. Unfortunately, there is no experimental measurement of T_e profile for this shot. Quite recently, the same behavior of T_e profile has been reported in JT-60U[8] by the reciprocating probe measurement. Similar "second SOL" was observed for similar discharge conditions (L-mode discharge with I_p=1.8MA, B_t=3.5T, q_{eff}=4.7), but higher density regime ($\bar{n}_e$=1.9-4.3x10^{19}m^{-3}) and lower input power(P_{NBI}=4MW). Temperature decay length l_T for the first SOL in Fig.5 becomes (a) l_T=0.5cm and (b) l_T=1.7cm, respectively, while 2.2-2.5cm in the above experiments. Density profiles are shown in Fig.6. Unlike the T_e profile, there is no "second SOL". In the above experiments[8], a "second SOL" has been also observed for n_e profile. In addition, the typical density decay length for the first SOL became 1.4cm-1.7cm. Density decay lengths in Fig.6 are apparently larger than these values. We have also used smaller D [case (c):D=0.5m^2/s in Sec.2]. However, we couldn't obtained such a drastic change to explain the above experimental observations, although l_n becomes smaller. Comparison with these recent experimental findings suggests that some different model of radial transport (for example, including pinch effect in the model) is necessary to

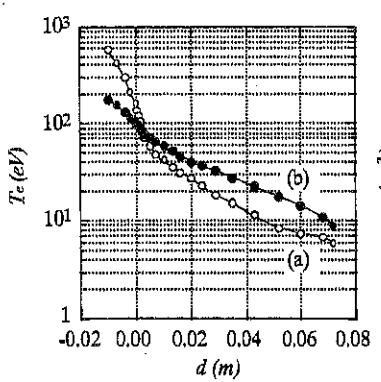

Fig.5 Te-Profile at outer mid-plane.

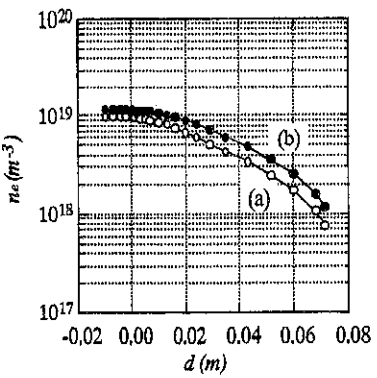

Fig.6 ne-profile at outer mid-plane

simulate JT-60U SOL and divertor plasmas. Figure 7 shows CII-line intensity for each channel of sight lines in Fig.1. Solid line is "B2-Eirene" result for the case(b) in Sec.2, while closed circles are experimental results from Ref.[6]. CII-line intensity profile of the numerical result is broader than the experimental result. This feature is related to the broad density profile in the SOL discussed above. Comparison of CII-line intensity profile here again suggests that more wide range and systematic study for the radial particle transport, together with the recycling property, will be needed in the future. In addition, peak value of the numerical results about 2.5 times larger than that of experimental results. As pointed out in

Ref.[6], chemical sputtering is important, not only in the high density regime, where physical sputtering is relatively less important, but also in the low density regime as in the present study. Shimizu, *et al*[6] found that only 10% of target-produced CD_4 reaches C^+, taking into account methane dynamics. Also in Ref.[9], with the use of the Monte-Carlo DIVIMP code, it has been shown that chemically sputtered hydrocarbons only contributes 10% of C^+ to explain the observed CII-line intensity profile. "B2-Eirene" code can take into account methane dynamics. However, in the present study, slow C-atoms launch at the target with the given chemical sputtering yield as in the Ref.[9]. Thus, we have implicitly assumed that 100% of hydrocarbon contribute to C^+ generation and it may be possible to overestimate C^+concentration. To examine this, a simple test calculation, in which chemical sputtering yield at the plate is set to be zero, has been done. The result is shown by dotted line in Fig.7. Although the profile is still broad, its peak value well agrees with the experimental result.

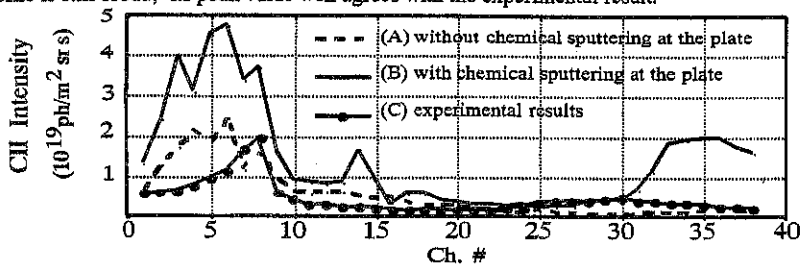

Fig.7 CII line intensity profiles

5. Summary Dependence of total particle flux at the plate on the upstream n_e has been compared with the experimental result in Ref.[5]. "B2-Eirene" results reproduce the essential feature in the experiments. Effects of the radial transport and chemical sputtering on the numerical results are also studied, taking shot#E19059[6] as an example. A clear 2nd SOL of T_e-profile has been observed in the simulation as in the recent experiment[8]. Decay length of 1st SOL almost agrees with the experimental value of Ref.[8] for χ_e=2.0m^2/s. However, to explain experimental n_e-profile, smaller D-value or different model of radial transport (ex. pinch effect) seems to be necessary. More systematic and wide range of parameter survey is now going on. Comparison of CII-line intensity suggests that only a small fraction of target-produced CD_4 can reach C^+ to explain the observed CII-line intensity. This "B2-Eirene" result supports the result in Ref.[6] by IMPMC Monte-Carlo code for impurity transport.

Acknowledgment The authors would like to thank Drs. D.Reiter, H.P.Zehrfeld, B.Braams and K.Borrass for their useful discussions. One of the authors (A.H.) gratefully acknowledge Prof. Lackner and Dr. Neuhauser for their encouragement during his stay at IPP Garching.

References

[1] R.Schneider, D.Reiter, H.P.Zehrfeld, B.Braams, *et al*: J.Nucl.Mater., 196-198(1992)810.
[2] B.Braams: NET report No.68 (EUR-FU/XII-80/87/87/68), 1987.
[3] D.Reiter: J.Nucl.Mater., 196-198(1992)80.
[4] D.Reiter, *et al*: Plasma Physics and Controlled Fusion, 33(1991)1579.
[5] N.Asakura, *et al*: Nucl.Fusion 35(1995)381.
[6] K.Shimizu, *et al*: *Plasma Physics and Controlled Fusion Research*, 1994, Vienna, IAEA 1995, Vol.2, p.431.
[7] F.Wagner and K.Lackner : in *Physics of Plasma Wall Interaction in Controlled Fusion*, p.931, Plenum, 1986.
[8] N.Asakura, *et al*: J.Nucl.Mater. 241-243(1997)559.
[9] H.Y.Guo, *et al*: *Proc. 22nd EPS Conf. on Contr. Fusion and Plasma Phys.*, Part II, p.273, 1995.